




RESEARCH ARTICLE OPEN ACCESS

Adolescent White Matter Maturation Mediates Epigenetic Associations With Cognitive Development

Dawn Jensen^{1,2}  | Jiayu Chen^{1,3} | Jessica A. Turner⁴ | Julia M. Stephen⁵  | Yu-Ping Wang⁶ | Tony W. Wilson⁷  | Vince D. Calhoun^{1,2,3,5,8} | Jingyu Liu^{1,3}

¹Tri-Institutional Center for Translational Research in Neuroimaging and Data Science (TReNDS): (Georgia State University, Georgia Institute of Technology, and Emory University), Atlanta, Georgia, USA | ²Neuroscience Institute, Georgia State University, Atlanta, Georgia, USA | ³Department of Computer Science, Georgia State University, Atlanta, Georgia, USA | ⁴Department of Psychiatry and Behavioral Health, Ohio State University, Columbus, Ohio, USA | ⁵The Mind Research Network, Albuquerque, New Mexico, USA | ⁶Department of Biomedical Engineering, Tulane University, New Orleans, Louisiana, USA | ⁷Institute for Human Neuroscience, Boys Town National Research Hospital, Boys Town, Nebraska, USA | ⁸Psychology Department and Neuroscience Institute, Georgia State University, Atlanta, Georgia, USA

Correspondence: Dawn Jensen (djensen2@gsu.edu)

Received: 19 July 2024 | **Revised:** 11 July 2025 | **Accepted:** 6 November 2025

Keywords: adolescent development | cognition | diffusion tensor imaging (DTI) | methylation | neuroimaging epigenetics | white matter

ABSTRACT

One hallmark of brain maturation in adolescence is increased myelination (fractional anisotropy [FA]) of the axons, although the epigenetic drivers of this stage of neurodevelopment are as yet poorly understood. Our previous study of a longitudinal cohort of normally developing adolescents, aged nine to fourteen, established the connections between changes in DNA methylation (DNAm) at seven cytosine–phosphate–guanine (CpG) sites in genes highly expressed in the brain to grey matter maturation as well as cognitive improvement. Continuing that work, we investigate the relationships between the changes in DNAm of these genes (*GRIN2D*, *GABRB3*, *KCNKI*, *SLC12A9*, *CHD5*, *STXBP5*, and *NFASC*), four networks of FA change, and scores from seven cognitive tests. The demethylation of the CpGs over time was significantly related to a brain network highlighting FA increases in regions associated with maturation of interhemispheric connectivity. Mediation analysis found that this same network mediated the relationship between decreases in DNAm of four of these genes and increases in overall cognitive performance. These relationships suggest that changes in DNAm of genes involved in myelination and the excitatory/inhibitory balance in the brain might be driving maturation of white matter, which in turn is implicated in the improved cognitive performance seen in adolescents.

1 | Introduction

Although adolescence is well-understood to be a phase of human neurodevelopment characterized by reorganization of the brain leading to improved cognitive function (Steinberg 2005), little is known about the underlying epigenetic mechanisms that may be driving these diverse and profound changes.

Epigenetic regulation of gene expression is both highly plastic and responsive to developmental cues (Dupont et al. 2009).

Animal studies point to large-scale epigenomic changes related to brain development that occur during adolescence (Mychasiuk and Metz 2016). Human research in epigenetic mechanisms involved in brain development had been restricted to the fetal brain due to the prior need to directly analyze brain tissue (Schneider et al. 2016). Advancements in epigenomics have made it possible to study epigenetic mechanisms involved in brain and cognitive development using peripheral tissue samples, such as DNA methylation (DNAm) biomarkers found in blood or saliva (Wheater et al. 2020; Walton et al. 2016; Lin et al. 2018;

This is an open access article under the terms of the [Creative Commons Attribution-NonCommercial](https://creativecommons.org/licenses/by-nc/4.0/) License, which permits use, distribution and reproduction in any medium, provided the original work is properly cited and is not used for commercial purposes.

© 2025 The Author(s). *Developmental Neurobiology* published by Wiley Periodicals LLC.

Proskovec et al. 2020). DNAm, which occurs when a methyl group is attached to a cytosine pyrimidine (CpG) ring in the DNA (Mangiavacchi et al. 2023; Moore et al. 2013; Perri et al. 2017), is one of several mechanisms that regulates gene expression. This can lead to either an increase or decrease in gene expression, when, for example, DNAm at a promoter region restricts expression by reducing overall transcription, or by causing alternative splicing during transcription (Dupont et al. 2009).

DNAm biomarkers in saliva and blood have been directly associated with DNAm in brain tissues (Braun et al. 2019; Han et al. 2019), as well as indicatively in both structural and functional aspects of the brain (Walton et al. 2016; Lin et al. 2018; Proskovec et al. 2020; Braun et al. 2019). In particular, one study, with 27 subjects, established the epigenome-wide correlation across tissue types that include resected brain tissue as well as saliva, blood, and buccal samples to be as high as 0.90 (Braun et al. 2019). Individual CpG sites that also had high correspondence across tissue-types (Braun et al. 2019). This advance in the field has made investigating the epigenomic mechanisms and their relationships to the brain across the lifespan much more feasible (Wheater et al. 2020). One of the few studies focused on adolescent development, published in 2019, found that roughly 15k CpGs showed significant changes in DNAm in blood pre and postadolescence when looking at a population across the span of 10–18 years of age (Han et al. 2019). A cross-sectional study from 2021 found relationships between symptoms of depression and childhood adversity were mediated by DNAm markers in blood (Smith et al. 2021).

Our own previous research established significant associations between DNAm changes in saliva at seven CpGs and grey matter maturation as well as cognitive development during adolescence (Jensen et al. 2023). The genes experiencing longitudinal change in DNAm in that study, *GRIN2D*, *GABRB3*, *KCNK1*, *SLC12A9*, *CHD5*, *STXBP5*, and *NFASC*, were originally selected based on their expression levels in the brain and were found to be involved in excitatory and inhibitory signaling, as well as myelination, synaptic vesicles, potassium channels, and histone regulation (Jensen et al. 2023). To continue to expand this small body of research concerning the effects that methylation has on normal adolescent brain and cognitive development (Wheater et al. 2020), our current research is focused on discovering and specifying the role change in the DNAm of these seven CpGs might play in white matter maturation, as measured by changes in fractional anisotropy (FA).

During adolescence, increases in FA, as measured by diffusion MRI, are seen from the onset of adolescence through early adulthood (Bava et al. 2010). FA is a measurement considered to reflect, indirectly, axonal integrity, myelination, and axon density of neurons in the brain (Bava et al. 2010). Several longitudinal studies have shown that increases in FA are associated with the maturation of the white matter tracts in adolescence beginning with the sensorimotor connections and is then followed by the frontocortical and frontosubcortical projection tracts, with further maturation then occurring in the corticolimbic association tracts and regional termination zones in the cortical and basal ganglia regions in early adulthood (Bava et al. 2010; Simmonds et al. 2014; Peters et al. 2012). The increases in FA that occur during adolescence are associated with improvements in

cognitive performance that include cognitive control (Simmonds et al. 2014), as well as improved performance in complex attention tasks, working memory, and verbal fluency (Peters et al. 2012).

Our study uses data collected from the Developmental Chronecto-Genomics (Dev-CoG): A Next Generation Framework for Quantifying Brain Dynamics and Related Genetic Factors in Childhood. This research study of a longitudinal cohort of around 200 typically developing subjects aged 9–14 collected, across three time points approximately 1 year apart, data that included neuroimaging measures, cognitive assessments, and saliva for DNAm (Stephen et al. 2021). Using the seven CpGs of interest from our previous research (Jensen et al. 2023), we will now assess their relationship with FA during adolescence maturation. To this end, we investigated the longitudinal relationship between DNAm and networks of FA increases over time using repeated measures linear mixed effects models, as well as a multilevel mediation analysis to explore the possibility these networks of FA increases may mediate the relationship between DNAm and cognition. We also used a multivariate analysis of covariance to investigate the relationship between the rates of change in DNAm and the FA networks by directly analyzing the differences between time points. Our current understanding of neural development, cognition, and epigenetics leads us to expect that increases in FA will be associated with the decreases in DNAm of six of the seven CpGs located on genes that are involved in excitatory and inhibitory systems in the brain and myelination. These networks of white matter maturation should also have a mediating effect on the relationship between these DNAm changes and cognitive development.

2 | Methods

2.1 | Cohort

The same cohort of subjects from our previous work (Jensen et al. 2023) was used in this analysis, recruited at the Mind Research Network (MRN) and the University of Nebraska Medical Center (UNMC) as part of the Dev-CoG study (Stephen et al. 2021), approved by the relevant institutional review board at each data collection site (Advarrra IRB—MRN and UNMC IRB—Nebraska). Data sharing was written into the consent forms and the study protocols (Stephen et al. 2021). The inclusion criteria for the study were English speaking, age 9–14 years at enrollment and both child and parent were able and willing to assent/consent to the study. The exclusion criteria for the study were current pregnancy, unable to consent/assent, history of developmental delays or disorders (or an individual education plan indicative of a developmental delay/disorder), history of epilepsy or other neurological disorders, parental history of major psychiatric or neurological disorder, self-reported prenatal exposure to alcohol or drugs, medication use, contraindication to MRI (MRI screening form was reviewed), or metal orthodontia (e.g., braces or spacers) (Stephen et al. 2021). Images, saliva samples, and cognitive tests were collected from 200 participants over three time points, roughly a year apart. See Table 1 for demographic information. Due to participant dropout during longitudinal data collection, our different analyses have different sample sizes. The flexibility of the linear mixed-effects model when dealing with missing data (Pinheiro and Bates 2000) allowed us to include 100

TABLE 1 | General demographic information: MRN—Mind Research Network, UNMC—University of Nebraska Medical College, BIPOC—Black, Indigenous, and People Of Color, WASI II IQ—Wechsler Abbreviated Scale of Intelligence, a general IQ test, a score between 90 and 102 is considered average, SES—socioeconomic score.

Demographics	MRN (101)	UNMC (102)
Mean age at enrollment (range)	11.3 (9–14)	11.2 (9–14)
Gender (M/F)	51M/50F	51M/51F
Race (Caucasian/BIPOC)	86/15	87/15
Ethnicity (% Hispanic)	41.6%	7.8%
Mean WASI-II IQ (range)	108.6 (72–139)	112.1 (68–148)
Mean SES (range)	42.6 (17–66)	48.2 (15–65)

subjects (45 girls, 55 boys, mean baseline age of 11.75 years old) in the repeated measures modeling reported below. The same subject set was used for the multilevel mediation analysis. The multivariate analyses of differences between time points included 145 subjects (mean baseline age 11.71 years old, 75 females, 70 males) for time points 1 and 2, and 82 subjects (37 females, 45 males) for time points 2 and 3.

2.2 | DNAm Preprocessing

The preprocessing largely followed the ENIGMA epigenetics protocol and was used in our previous study (Jensen et al. 2023). DNAm from saliva was assessed for each subject using the Illumina HumanMethylation850 (850k) microarray, which measures CpG methylation across ~850,000 probes covering CpG islands, shores, and shelves; 5'UTR, 3'UTR, and bodies of RefSeq genes; and promoters and enhancer regions. Standardized quality control procedures and quantile normalization were performed using the minfi Bioconductor package in R (version 3.6.2) (Aryee et al. 2014). Red and green channel intensities were mapped to the methylated and unmethylated status; samples were checked against the mean intensity to identify low quality. Beta values, calculated for each CpG, for each subject, reflect the degree of methylation using a range of zero, meaning no methylation, to one, meaning completely methylated. To identify outliers, a principal component analysis (PCA) was performed on the beta values. Any sample with values more than three standard deviations away from the median on any of the first four components was removed, as were samples where the genetically determined sex differed from self-report. Twenty duplicate DNA samples were included in each batch and checked to ensure measurement reliability. Samples processed in different batches were merged at this stage. Stratified quantile normalization was then applied across samples, using the minfi PreprocessQuantile function. The cell proportions for each DNAm sample were calculated by implementing the estimateCellCounts function in minfi, using our modified reference panel of five types of blood cells (B cells, CD8T and CD4T cells, NK-LGL cells, monocytes, and granulocytes) and epithelial cells (GSE46573) (Aryee et al. 2014). The proportion of total blood cells and epithelial cells was strongly in alignment with EpiDISH (Zheng et al. 2018) estimated immune cells and epithelial cells (correlation >0.98). The cell type effect was regressed out from all the samples to account for the change of cell proportion over time. Batch effects then were corrected using the R package Combat, which assumes

normalized data and equalizes the mean from all batches, making negative values possible (Johnson et al. 2007).

2.3 | CpG Selection

We applied the same CpG selection as our previous study (Jensen et al. 2023). In brief, after preprocessing, approximately 750k CpG sites were retained. We kept only CpG sites with a standard deviation of 0.1 or higher at the first time point to ensure that methylation variability across subjects exceeded measurement variability (Duan et al. 2021). Then, paired *t*-tests between time points were used to further filter the CpGs to only those showing significant changes in methylation. After FDR correction, 54 CpG sites during deltaT1 (time point 2 [TP2]–time point 1 [TP1]) and 465 CpGs during deltaT2 (time point 3 [TP3]–TP2) showed significant changes in DNAm. Fifty of these CpGs were in common between all three time points. Seven of these CpGs were found to be located on genes highly expressed in the brain based on Human Protein Atlas (Andersson and Sotiropoulos 2016). Refer to Figure S1 for a diagram of the filtering process. The selected seven CpGs are cg01008256 (*SLC12A9*), cg23841819 (*NFASC*), cg01483824 (*GRIN2D*), cg15205435 (*CHD5*), cg14859324 (*GABRB3*), cg26703758 (*KCNK1*), and cg15866800 (*STXBP5*). Figure 1A–G highlights the change in DNAm across time observed in these seven genes. As published in our previous work (Jensen et al. 2023), six of these genes displayed decreases in DNA, across time (*SLC12A9*, *NFASC*, *GRIN2D*, *GABRB3*, *KCNK1*, and *STXBP5*). Only one gene, *CHD5*, experienced an increase in DNAm over all three time points (Jensen et al. 2023). The subsequent analyses focused on these seven CpG sites. See Tables S1–S3, and S6 for detailed information on these seven CpGs including difference between time points, gene set enrichment using g:Profiler (Raudvere et al. 2019), and basic gene functions.

2.4 | Diffusion

The diffusion-weighted (dMRI) images were collected at the MRN site on a Siemens 3T TrioTrim scanner, and at UNMC site on a Siemens 3T Magnetom Skyra and Prisma scanners, all with a 32-channel radio frequency coil (Stephen et al. 2021). Scanning parameters were AP/PA, at 2 × 2 × 2 mm resolution, *b* value 2400 s/mm², TR = 4000 ms, TE = 108 ms, 165 directions, and were equilibrated between sites as much as possible (Stephen et al. 2021). dMRI was collected with phase reversed blips, and *b*-

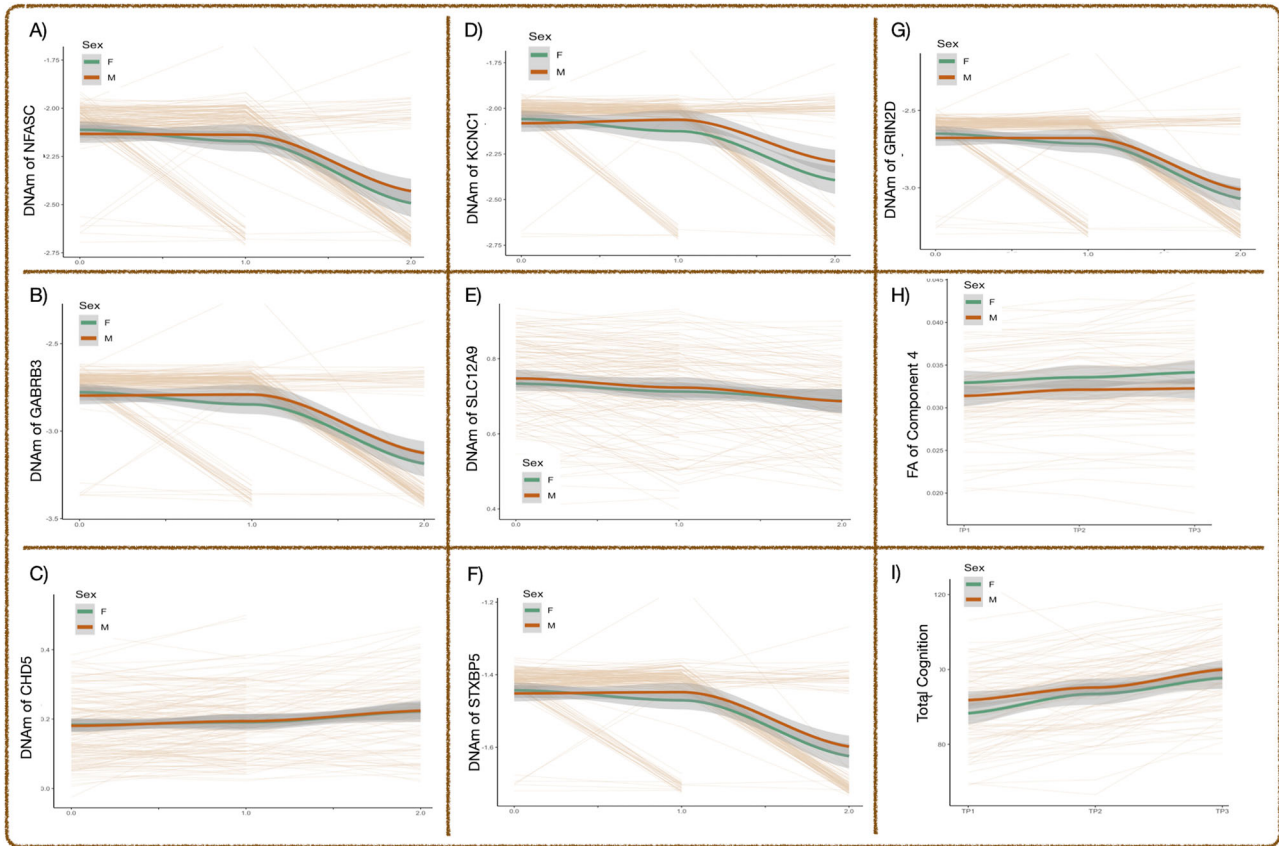


FIGURE 1 | Change across three time points. (A–G) DNAm tested for significant across time with two-sided *t*-tests, FDR-corrected *p* values—(A) DNAm of NFASC: T1–T2($t = -4.14, p < 0.004$), T2–T3($t = -12.38, p < 5.2 \cdot 10^{-20}$). (B) DNAm of GABRB3: T1–T2($t = -4.30, p < 0.003$), T2–T3($t = -9.35, p < 1.3 \cdot 10^{-13}$). (C) DNAm of CHD5: T1–T2($t = 3.57, p < 0.021$), T2–T3($t = 4.69, p < 1.4 \cdot 10^{-4}$). (D) DNAm KCNC1: T1–T2($t = -4.36, p < 0.003$), T2–T3($t = -13.44, p < 6.0 \cdot 10^{-21}$). (E) DNAm of SLC12A9: T1–T2($t = -4.87, p < 0.003$), T2–T3($t = -4.31, p < 5.3 \cdot 10^{-4}$). (F) DNAm of STXBP5: T1–T2($t = -4.36, p < 0.003$), T2–T3($t = -13.21, p < 6.2 \cdot 10^{-21}$). (G) DNAm of GRIN2D: T1–T2($t = -4.31, p < 0.003$), T2–T3($t = -13.05, p < 7.0 \cdot 10^{-21}$). (H and I) FA changes and cognitive scores across time (respectively) tested for significance using repeated measures mixed effects linear regression, Bonferroni tested for multiple comparisons—(H) FA of Component 4: T1–T2($t = 4.704, p < 4.78 \cdot 10^{-6}$), T2–T3($t = 7.04, p < 3.04 \cdot 10^{-11}$) (I) Scores from Total Cognition Composite: T1–T2($t = 9.12, p < 2.0 \cdot 10^{-16}$), T2–T3($t = 18.8, p < 2.0 \cdot 10^{-16}$). Green lines represent the mean of male subjects and orange lines represent the mean of female subjects. DNAm, DNA methylation; FA, fractional anisotropy.

zero volumes were extracted and used to estimate off resonance fields using FSL (v6.0.3) tool top up (Andersson et al. 2003; Smith et al. 2004). These were used to correct the diffusion tensor imaging (DTI) volumes for head movement, EPI distortions, and eddy current-induced distortions using FSL tool eddy (Andersson and Sotiropoulos 2016). Advanced motion correction was also performed in eddy to detect motion-induced signal dropout and intra-volume (slice-to-volume) movement (Andersson et al. 2017). Using the AFNI (v19.1.00) tool *3dDWItoDT*, FA maps were constructed (Taylor and Saad 2013). The DTI derivative images were reoriented and registered to a cohort-specific template, created using the ANTS multivariate template generator (Andersson et al. 2007a, 2007b; Sanchez et al. 2012; Avants et al. 2008). The resultant FA values then had the scanner differences regressed out using a simple linear regression that included age and sex as covariates. To calculate the rate and direction of change over time, the FA values from TP1 were subtracted from TP2 to create the deltaT1 difference map, and TP2 was subtracted from TP3 to create the deltaT2 difference map. An independent component analysis (ICA) built in the GIFT toolbox (SBM v1.0b) (Stephen et al. 2021) was then applied to the difference maps to extract

components/brain networks of interest, where distributed brain regions showed covarying patterns of longitudinal FA changes. Using the minimum description length (MDL) criterion (Cahoun and Adali 2009), four components were extracted from the FA changes in deltaT1, identifying our brain networks of interest for this study (see Figure 2A). These networks of interest were then used to “mask” the FA images at each of the three time points to ensure uniformity of comparison. The component-associated loadings reflect the variation of FA change networks across subjects. The direction of the ICA loadings was confirmed using the FSLmeants function to extract the average FA within the component networks, where positive loadings indicated increases in FA and negative loadings indicated decreases in FA. The spatial maps of these four components were projected onto the subjects’ deltaT2 FA images, as well as to the subjects’ FA images at each time point, to ensure uniformity of comparison. ICA component maps were projected into MNI space for anatomical atlas region identification. To assess significant change over time, a linear mixed-effects repeated measures regression (Zheng et al. 2018) with age and sex as covariates was performed on all four components. Only Comp4 showed significant change across all

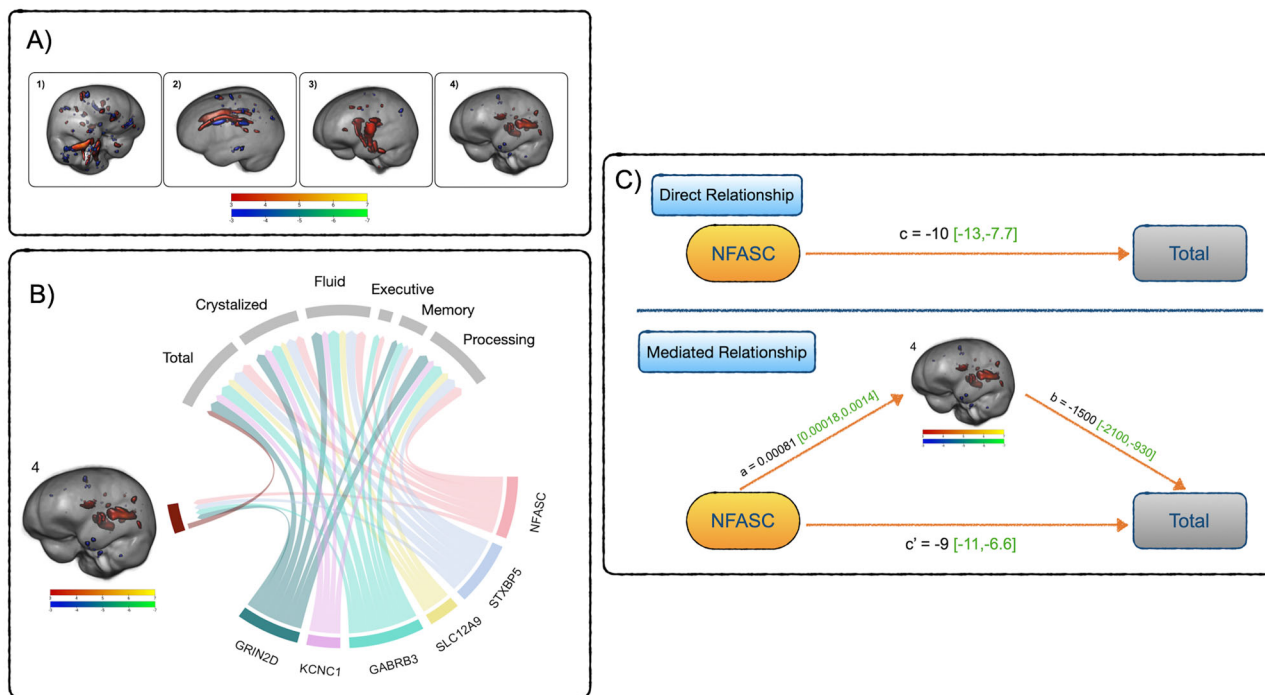


FIGURE 2 | Relationships between FA, DNAm, and cognition—(A) **FA ICA results**: Components 1–4, thresholded from $-7 < z < -3$ (blue to green) and from $3 < z < 7$ (red to yellow), highlighting covarying differences in FA. Blue–green are areas of FA decrease over time, red–yellow are areas of FA increase. See Table S5 for a comprehensive list of regions. (B) **Repeated measures results**: Summary of the significant relationships between FA (Comp4), DNAm, and cognitive performance across all three time points. The width of the links corresponds to the effect size (t -statistic) of the relationship (DNAm and Comp4—mean t -stat -2.77 , Comp4 and COGTC— t -stat 2.70 , DNAm, and cognition—mean t -stat -4.95). (C) **Direct and mediated relationship between NFASC and total cognition**: mediating effect of Comp4: $-1.2[-2.4, -0.22]$, percent mediated: 12% [2.3,23]. Cognitive measure labels: total—COGTC, crystallized—COGCC, fluid—COGFC, executive—TBDCCS, memory—TBPSM, and processing—PCPS.

three time points and was thus chosen for the repeated measures and mediation analyses mentioned later. This change across time can be seen in Figure 1H.

2.5 | Cognitive Data

The age-uncorrected standard scores from the following NIH cognitive toolbox tests (Denboer et al. 2014) were collected from each subject: the Picture Sequence Memory (TBPSM) test for 8+ (episodic memory), the Pattern Comparison Processing Speed (PCPS) test for 7+ (processing speed), the Flanker Inhibitory Control and Attention (TBFICA) test for 8+ (executive function), and the Dimensional Change Card Sort (TBDCCS) for 8+ (executive function). The Cognition Total Composite Score (COGTC), the Cognition Fluid Composite Score (COGFC) reflecting capacity for new learning, and the Cognition Crystallized Composite Score (COGCC) reflecting past learning were computed. Age-uncorrected scores were used to preserve the sensitivity to differences in age. Scores were corrected for site differences using a linear regression with age and sex as covariates. To calculate the rate of change across time points, scores from TP1 were subtracted from TP2 to create the deltaT1 difference map, and TP2 was subtracted from TP3 to create the deltaT2 difference map. As shown in our previous study (Jensen et al. 2023), linear mixed-effects repeated measures models confirmed the expected significant improvements in cognitive performance over time. This improvement was significantly related to decreases

in DNAm in six CpG sites (Jensen et al. 2023). Figure 11 highlights the change across time for the Total Composite Score. Comprehensive details for the cognitive scores can be found in Tables S3 and S4.

3 | Statistical Tests

3.1 | Repeated Measures Modeling to Investigate Longitudinal Change

A repeated measures mixed effects model (Pinheiro and Bates 2000) was used to test the relationship between the DNAm at each of the seven CpGs and the brain networks highlighted in Comp4 using the lme4 package in R (version 4.1.2) (Bates et al. 2015). The subjects' FA network loadings (representing the networks' variation across subjects) were the dependent variables and the DNAm measures of the seven CpGs were the independent variables. Sex and baseline age were included as fixed effects, whereas subject intercept and slope were included as random effects to account for individual variability as well as repeated measures (Singer and Willett 2003). Initially, a family variable was added as a random effect to account for the impact of siblings within the study but then removed from the model because it did not account for a significant amount of variance. The differing time intervals between subjects' data collection were also included as a possible confounder and ruled out. The repeated measures mixed effects model results were Bonferroni

corrected to control for Type I error at 5% resulting from seven tests (Etymologia: Bonferroni Correction 2015).

Similarly, a repeated measures mixed effects model was used to test the relationships between one FA network and each of the cognitive tests across all time points. In this model, the cognitive scores were the dependent variable and the subjects' loadings from the FA networks were the independent variables, whereas sex and baseline age were covariates. The results were Bonferroni corrected to control for Type I error at 5% (Etymologia: Bonferroni Correction 2015).

Visualization of Q–Q plots of the residual was used to check for violations of normative distribution and variance Feng 2020. All measures were checked for sphericity and collinearity. Outliers showed no effect on results. The mixed-effect repeated measures linear models were chosen for their robustness to violations of normality as a further safeguard [Gabrio 2022].

3.2 | Mediation Analysis

A multilevel mediation analysis was used to explore the relationships between the changes in DNAm and the improvement in cognitive performance across all three time points and if they might be mediated by the network of FA changes. Only measures that had significant results from the mixed-effects linear models that passed Bonferroni correction were tested in the multilevel mediation analysis, using a Bayesian inference engine from the `bmlm` package in R (Vuorre 2023) to estimate the indirect effect and percentage of mediated effect by the FA changes in the brain on the direct relationships of the methylation changes on cognitive performance. The cognitive changes were the dependent variable, the changes in DNAm the independent variable, the subject loadings from the FA network the mediator, and the three time points were the multiple levels. Confidence intervals were calculated using the indirect effects at the 2.5th and 97.5th percentiles (Vuorre 2023). Rhat values were proofed to ensure appropriate convergence and models where the confidence intervals for the Bayesian parameters crossed zero were not considered [].

3.3 | Multivariate Rates of Change Analysis

A multivariate analysis, MANCOVA, was conducted to explore the relationship between the rates and direction of change within the DNAm and FA. This was performed on data from deltaT1 and deltaT2 separately using the `jmv` package in R (version 4.1.2) (R: MANCOVA n.d.). The subjects' loadings from four FA networks from the difference maps as the dependent variables, the differences of DNAm in the seven CpGs as the independent variables, and sex and baseline age as the covariates. MANCOVA results were further tested with regression tests for each FA network for potential interactions with sex using the `emmeans` package in R (version 4.1.2) (`emmeans` function—RDocumentation n.d.).

Similarly, a multivariate analysis was used to explore the relationship between the rates and direction of change in the cognitive measures and FA. The MANCOVA analysis was performed on data from deltaT1 and deltaT2 separately, where differences in

cognitive scores were the dependent variables and the subjects' loadings from the FA networks from the difference maps were the independent variables, with sex and baseline age as covariates.

4 | Results

FA increased across networks of white matter tracts that include the corpus callosum, parietal, and temporal regions. The ICA identified four brain networks (referred to as components in Figure 2A) highlighting regions of FA changes within the subjects' brains over time. These regions were identified using the JHU DTI-based white-matter atlas (Mori et al. 2005; Wakana et al. 2007; Hua et al. 2008) as well as the Harvard–Oxford cortical and subcortical structural atlases (Makris et al. 2006; Frazier et al. 2005; Desikan et al. 2006, Goldstein et al. 2007) and the probabilistic cerebellar atlas (Diedrichsen et al. 2009). The first component (Comp1) highlights a network of FA increases in the middle cerebellar peduncle and white matter tracts in anterior fusiform gyrus, precentral gyrus, and angular gyrus covarying with decreases in FA in tracts in the bilateral cerebellum, inferior temporal gyrus, and frontal pole. The second (Comp2) highlights increases of FA in the anterior and posterior corona radiata, the body, splenium, and genu of the corpus callosum, and the posterior thalamic radiation that covaried with decreases in FA in the superior longitudinal fasciculus and white matter tracts in the superior frontal gyrus, the post central gyrus, and the posterior temporal gyrus. The third component (Comp3) consists of a network of increased FA in the middle cerebellar peduncle, the posterior limb of the internal capsule, the splenium of the corpus callosum, and the superior corona radiata. The fourth component (Comp4) is a network of FA increases in the splenium and body of the corpus callosum, the tapetum, the posterior thalamic radiation, as well as white matter tracts in the cuneus and superior lateral occipital cortices. See Table S5 for a detailed listing of the brain regions. Only one component, Comp4, showed significant change across all time points (TP1–TP2: $t = 4.71$, $p < 4.78^{-6}$, TP2–TP3: $t = 7.04$, $p < 3.04^{-11}$), so it was the only component used in the repeated measures longitudinal analysis. All four components were included in the multivariate rate of change analysis.

Increases in FA in the splenium and body of the corpus callosum as well as the posterior thalamic radiation were directly associated with increases in total cognitive performance and decreases in DNAm regulating genes involved in myelination as well as inhibitory and excitatory receptor subunits. To assess the longitudinal relationship between the network of increased FA highlighted in Comp4 and cognitive performance over time, a repeated measures linear mixed-effects analysis was performed. The network of FA highlighted in Comp4 was significantly related to COGTC ($t = 2.70$, $p < 0.008$). A similar repeated measures linear mixed effects model showed that increases in FA found in Comp4 were inversely related to decreases in DNAm at CpGs on *NEFASC* ($t = -2.72$, $p < 0.007$), *GRIN2D* ($t = -2.8$, $p < 0.006$), *STXBP5* ($t = -2.81$, $p < 0.006$), and *GABRB3* ($t = -2.76$, $p < 0.007$). These were relationships passed Bonferroni-correction (uncorrected $p < 0.008$). Figure 2B summarizes these results as well as the associations between DNAm and cognition reported in our previous study (Jensen et al. 2023), for completeness.

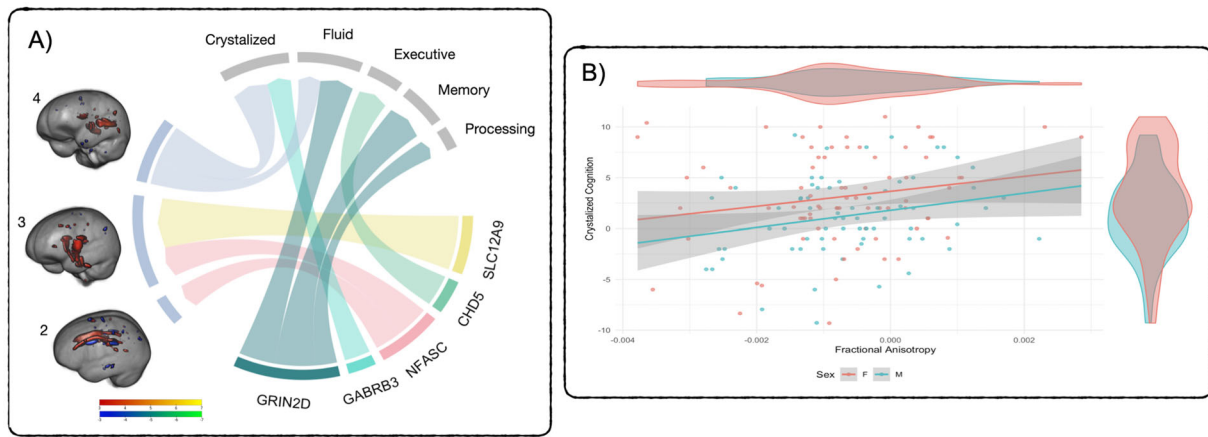


FIGURE 3 | Rates of change analysis—(A) MANCOVA results overview: Pictured are the significant relationships between the rates of change in FA, DNAm, and cognitive performance. The width of the links corresponds to the effect size (F-ratio) of the relationship. Only the relationships between Comp4 and crystallized and fluid cognition occurred during deltaT1. **(B) Rate of increasing FA in Comp4 related to the rate of improvement in crystallized cognition:** multivariate F -stat = 5.32, $p < 0.005$, univariate F -stat = 6.86, $p < 0.009$. Cognitive measure labels: crystallized—COGCC, fluid—COGFC, executive—TBDCCS, memory—TBPSM, and processing—PCPS.

Increases in FA in the splenium and body of the corpus callosum as well as the posterior thalamic radiation mediated the relationships between total cognitive improvement and the decreases in DNAm regulating genes involved in myelination as well as inhibitory and excitatory receptor subunits. As the total cognitive score was significantly associated with FA network in Comp4, multilevel mediation analyses were used to explore the mediation effect of FA Comp4 on the relationships between the improvement in the total cognitive performance and the decreases in DNAm. The Comp4 network of FA mediated the relationships between the decreases in DNAm of the CpGs on *NFASC* (mediated effect (me): $-1.2 [-2.4, -0.22]$, percent mediated effect (pme): 12% [2.3, 23]), *GRIN2D* (me: $-1.1 [-2.1, -0.23]$, pme: 11% [2.5, 22]), *STXBP5* (me: $-2.5 [-4.8, -0.56]$, pme: 11% [2.6, 21]), and *GABRB3* (me: $-1.1 [-2.1, -0.21]$, pme: 10% [2.2, 20]) and the improvements in COGTC. Figure 2C highlights the Comp4-mediated relationship between decreases in DNAm at *NFASC* and total cognitive scores.

There were diverse relationships between rates of change in FA networks and rates of cognitive improvement, as well as rates of change in DNAm at several CpGs. The relationship between the rates of change in FA networks, cognition, and DNAm was investigated using MANCOVA analyses. The Comp4 FA network shown in Figure 3A (multivariate $F = 5.32$, $p < 0.005$) was associated with the rates of increase in COGFC (univariate $F = 4.28$, $p < 0.04$) and COGCC (univariate $F = 6.86$, $p < 0.009$) during deltaT1, which was highlighted in Figure 3B. There were no significant relationships between the rates of change in DNAm and FA in deltaT1. There were significant relationships between the rate of change in DNAm of *NFASC* (multivariate $F = 2.89$, $p < 0.02$) and the rates of FA change in Comp2 (univariate $F = 4.81$, $p < 0.03$) and Comp3 (univariate $F = 5.88$, $p < 0.01$) in deltaT2. There were significant relationships between the rate of change in DNAm of *SLC12A9* (multivariate $F = 2.68$, $p < 0.03$) and the rate of FA change in Comp3 (univariate $F = 9.82$, $p < 0.002$) in deltaT2. Figure 3A is an overview of the results of the multivariate analyses as well as the associations between rates of change in

DNAm and cognition reported in our previous study (Jensen et al. 2023), for completeness.

5 | Discussion

Our previous research, looking at a cohort of normally developing adolescents, established that decreases in the DNAm at CpG sites located on *SLC12A9*, *NFASC*, *GRIN2D*, *STXBP5*, *GABRB3*, and *KCNKI* were associated with increases in multiple cognitive measures, as well as grey matter maturation (Jensen et al. 2023). Our current study has expanded our understanding of how decreases in DNAm in these genes, which play parts in the excitatory and inhibitory signaling of the brain as well as the regulation of myelination (Gagnon and Delpire 2013; Williams et al. 2011; Caballero and Tseng 2016; Wenzel et al. 1996; PubChem n.d.; Suzuki et al. 2017), are related to white matter maturation. It also offers some insight into how development of the brain may be mediating the relationships between the decreases in methylation and the improvements in cognition over time. The function and roles of these individual genes in the brain have been summarized in Jensen et al. (2023) and also provided in Table S6. The gene-enrichment pathway analysis from g:Profiler (Raudvere et al. 2019) shows that these genes are involved in pathways that are responsible for the regulation of presynaptic membrane potential, the postsynaptic membrane, the main axon, receptor complexes, and the hippocampal mossy fiber to CA3 synapse.

The networks of FA change identified in this cohort align with the current understanding of their stage of development. FA increases dynamically from birth on, with the largest increases occurring in the first 3 years, a tapering off around 5 years of age, and then a second, but more modest phase of increases that starts in adolescence and continues well into the third decade of life Lebel 2018. Longitudinal research has shown that, during adolescence, this maturation process is differentiated across tracts, following both the changes in grey matter volume and connectivity related to the transition to adulthood (Bava

et al. 2010). Several of the major white matter networks mature earlier in adolescence (Bava et al. 2010). These include projection tracts responsible for cortical/subcortical connection, inter hemispheric callosal fibers, cerebellar white matter, and longer range cortico-cortical association tracts (Bava et al. 2010). The major frontal and limbic tracts, in contrast, do not reach peak maturation until the second and third decades of life, with some experiencing a lull in growth during early adolescence (Bava et al. 2010). Our study identified networks of white matter maturation in the projection tracts, callosal tracts, and the beginnings of maturation of the association tracts. Our study did not identify significant increases in FA across time within the limbic tracts. This could be due to their stage of maturation (Bava et al. 2010) or the diversity of ages within our study. The network of significant FA increases highlighted in Comp4, which includes the splenium and body of corpus callosum, the tapetum, and the posterior thalamic radiation, as well as white matter within the cuneus and lateral superior occipital cortices, was related to the improvements in total cognition as well as the rates of improvement in the crystallized and fluid cognition. Increases in FA in these areas of the brain are linked to improved interhemispheric interactions, as well as increased efficiency in recruitment of neural populations (Knyazeva 2013). These changes lead to enhanced activation and more coordinated inhibition within the brain (Knyazeva 2013) and are associated with improvements in executive function, response inhibition, and working memory (Simmonds et al. 2014; Peters et al. 2012).

Interestingly, the network of FA increases highlighted in Comp4 was also significantly related to the decreases in DNAm across time in *GRIN2D*, *GABRB3*, *STXBP5*, and *NFASC*. This particular network, highlighting maturation of interhemispheric connectivity (Knyazeva 2013) of white matter in the brain, mediated the relationships between the decreases in DNAm of those same four genes and the improvement in total cognitive performance seen at this stage of development. This suggests that at least some of relationship between the pathways that these genes are enriched in, the regulation of presynaptic membrane potential, the postsynaptic membrane, the main axon, receptor complexes, and the hippocampal mossy fiber to CA3 synapse are impacting cognition through the role they play within the maturation of white matter. For example, *GRIN2D* and *STXBP5* are both directly involved in excitatory neurotransmission (Wenzel et al. 1996; Zanini et al. 2016). GABAergic network maturation is implicated in the restructuring of the hippocampus and is linked to improvements in executive function (Schmidt-Wilcke et al. 2018; Caballero and Tseng 2016). Increases in FA could be related to the demethylation of *NFASC*, which regulates myelination (Klingseisen et al. 2019).

The rates of white matter maturation in two other brain networks, highlighting FA increases in callosal and projection tracts, were related to the rate of decrease in DNAm in *NFASC* and *SLC12A9* during deltaT2. These relationships, while more diverse, may be less consistent due to the dynamic nature of rates of change, which may be more sensitive to the different stages of puberty.

One of the limitations of this study is that no measure for pubertal stage was collected. Including this marker for hormonal change during adolescence in future studies would further complete the model. Loss of subjects by the third time point reduced the

number of subjects with complete data. Due to this limitation, this study should be considered preliminary and future work should include more subjects. A further limitation to this work is the as-yet incomplete understanding of the downstream regulation effects of changes in DNAm on these genes. Gene expression generally decreases when DNAm increases, and vice versa, but not universally (Dupont et al. 2009). These results highlight a variety of future directions for further study of these seven CpGs, including how changes in DNAm effect expression of these genes within the brain. Future work will include an epigenome-wide investigation of the cohort to reveal the broader effects of changes in DNAm on adolescent brain and cognitive development.

6 | Conclusion

Our novel research has highlighted the intricacies of epigenetic changes and their relationship to maturation of white matter during adolescence. We also showed that during this early phase of white matter maturation, FA increases in brain networks involved in interhemispheric connectivity are related to the decreases in methylation of genes enriched in pathways that involve the regulation of presynaptic membrane potentials, the postsynaptic membranes, the main axons, receptor complexes, as well as the hippocampal mossy fiber synapses and overall cognitive improvement across time. This same network of white matter maturation also mediates the relationship between the demethylation of these genes and improvements in overall cognitive performance during adolescence. These findings offer new research directions from which a more detailed understanding of the molecular underpinnings of the drivers of adolescent brain development may emerge.

Author Contributions

Dawn Jensen: writing, editing, analysis. **Jiayu Chen:** writing, analysis, editing. **Jessica A. Turner:** supervision, editing. **Julia M. Stephen:** data collection, editing. **Yu-Ping Wang:** data collection, editing. **Tony W. Wilson:** data collection, editing. **Vince D. Calhoun:** data management, financial support, editing. **Jingyu Liu:** supervision, financial support, editing.

Acknowledgments

This research was supported by grants R01-MH121101, P20-GM144641, P30-GM122734, P50-AA22534, R56-MH124925, and R01-MH118695 from the National Institutes of Health and grants 1539067 and 2112455 from the National Science Foundation grant 2316421. The funders had no role in study design, data collection, analysis, decision to publish, or manuscript preparation. We want to thank the participants for volunteering to participate in the study and our staff and local collaborators for contributing to the work.

Ethics Statement

This study was approved by the Advarrra IRB at the Mind Research Network (MRN) and the University of Nebraska Medical Center (UNMC) IRB in Nebraska as part of the Dev-CoG study (Stephen et al. 2021).

Conflicts of Interest

The authors declare no conflicts of interest.

Data Availability Statement

The data that support the findings of this study are available on request from the corresponding author. The data are not publicly available due to privacy and ethical restrictions.

References

- Andersson, J. L. R., M. S. G. I. Drobnyak, H. Zhang, N. Filippini, and M. Bastiani. 2017. "Towards a Comprehensive Framework for Movement and Distortion Correction of Diffusion MR Images: Within Volume Movement." *Neuroimage* 152: 450–466.
- Andersson, J. L. R., M. Jenkinson, and S. Smith. 2007a. *Non-Linear Optimisation*. FMRIB Technical Report TR07JA1. FMRIB.
- Andersson, J. L. R., M. Jenkinson, and S. Smith. 2007b. *Non-Linear Registration Aka Spatial Normalization*. FMRIB Technical Report TR07JA2. FMRIB.
- Andersson, J. L. R., S. Skare, and J. Ashburner. 2003. "How to Correct Susceptibility Distortions in Spin-Echo Echo-Planar Images: Application to Diffusion Tensor Imaging." *Neuroimage* 20, no. 2: 870–888.
- Andersson, J. L. R., and S. N. Sotiropoulos. 2016. "An Integrated Approach to Correction for Off-Resonance Effects and Subject Movement in Diffusion MR Imaging." *Neuroimage* 125: 1063–1078.
- Aryee, M. J., A. E. Jaffe, H. Corrada-Bravo, et al. 2014. "Minfi: A Flexible and Comprehensive Bioconductor Package for the Analysis of Infinium DNA Methylation Microarrays." *Bioinformatics* 30, no. 10: 1363–1369.
- Avants, B. B., C. L. Epstein, M. Grossman, and J. C. Gee. 2008. "Symmetric Diffeomorphic Image Registration With Cross-Correlation: Evaluating Automated Labeling of Elderly and Neurodegenerative Brain." *Medical Image Analysis* 12, no. 1: 26–41. <https://doi.org/10.1016/j.media.2007.06.004>.
- Bates, D., M. Mächler, B. Bolker, and S. Walker. 2015. "Fitting Linear Mixed-Effects Models Using lme4." *Journal of Statistical Software* 67, no. 1: 1–48. <https://doi.org/10.18637/jss.v067.i01>.
- Bava, S., R. Thayer, J. Jacobus, M. Ward, T. L. Jernigan, and S. F. Tapert. 2010. "Longitudinal Characterization of White Matter Maturation During Adolescence." *Brain Research* 1327: 38–46.
- Braun, P. R., S. Han, B. Hing, et al. 2019. "Genome-Wide DNA Methylation Comparison Between Live Human Brain and Peripheral Tissues Within Individuals." *Translational Psychiatry* 9, no. 1: 1–10.
- Caballero, A., and K. Y. Tseng. 2016. "GABAergic Function as a Limiting Factor for Prefrontal Maturation During Adolescence." *Trends in Neurosciences* 39, no. 7: 441–448. <https://doi.org/10.1016/j.tins.2016.04.010>.
- Caballero, A., and K. Y. Tseng. 2016. "GABAergic Function as a Limiting Factor for Prefrontal Maturation During Adolescence." *Trends in Neurosciences* 39, no. 7: 441–448. <https://doi.org/10.1016/j.tins.2016.04.010>.
- Calhoun, V. D., and T. Adali. 2009. "Feature-Based Fusion of Medical Imaging Data." *IEEE Transactions on Information Technology in Biomedicine* 13, no. 5: 711–720. <https://doi.org/10.1109/TITB.2008.923773>.
- Denboer, J. W., C. Nicholls, C. Corte, and K. Chestnut. 2014. "National Institutes of Health Toolbox Cognition Battery." *Archives of Clinical Neuropsychology* 29, no. 7: 692–694.
- Desikan, R. S., F. Ségonne, B. Fischl, et al. 2006. "An Automated Labeling System for Subdividing the Human Cerebral Cortex on MRI Scans Into Gyral Based Regions of Interest." *Neuroimage* 31, no. 3: 968–980.
- Diedrichsen, J., J. H. Balster, E. Cussans, and N. Ramnani. 2009. "A Probabilistic MR Atlas of the Human Cerebellum." *Neuroimage* 46, no. 1: 39–46.
- Duan, K., A. R. Mayer, N. A. Shaff, et al. 2021. "DNA Methylation Under the Major Depression Pathway Predicts Pediatric Quality of Life Four-Month Post-Pediatric Mild Traumatic Brain Injury." *Clinical Epigenetics* 13, no. 1: 140. <https://doi.org/10.1186/s13148-021-01128-z>.
- Dupont, C., D. R. Armant, and C. A. Brenner. 2009. "Epigenetics: Definition, Mechanisms and Clinical Perspective." *Seminars in Reproductive Medicine* 27, no. 5: 351–357.
- "Emmeans Function—RDocumentation." n.d. <https://www.rdocumentation.org/packages/emmeans/versions/1.8.2/topics/emmeans>.
- "Etymologia: Bonferroni Correction." 2015. *Emerging Infectious Diseases* 21, no. 2: 289. <https://doi.org/10.3201/eid2102.ET2102>.
- Feng, C., L. Li, and A. Sadeghpour. 2020. "A comparison of residual diagnosis tools for diagnosing regression models for count data." *BMC Medical Research Methodology* 20: 175. <https://doi.org/10.1186/s12874-020-01055-2>.
- Frazier, J. A., S. Chiu, J. L. Breeze, et al. 2005. "Structural Brain Magnetic Resonance Imaging of Limbic and Thalamic Volumes in Pediatric Bipolar Disorder." *American Journal of Psychiatry* 162, no. 7: 1256–1265.
- Gabrio, A., C. Plumpton, S. Banerjee, and B. Leurent. 2022. "Linear mixed models to handle missing at random data in trial-based economic evaluations." *Health Economics* 31, no. 6: 1276–1287.
- Gagnon, K. B., and E. Delpire. 2013. "Physiology of SLC12 Transporters: Lessons From Inherited Human Genetic Mutations and Genetically Engineered Mouse Knockouts." *American Journal of Physiology—Cell Physiology* 304, no. 8: C693–C714. <https://doi.org/10.1152/ajpcell.00350.2012>.
- Goldstein, J. M., L. J. Seidman, N. Makris, et al. 2007. "Hypothalamic Abnormalities in Schizophrenia: Sex Effects and Genetic Vulnerability." *Biological Psychiatry* 61, no. 8: 935–945.
- Han, L., H. Zhang, A. Kaushal, et al. 2019. "Changes in DNA Methylation From Pre- to Post-Adolescence Are Associated With Pubertal Exposures." *Clinical Epigenetics* 11, no. 1: 176. <https://doi.org/10.1186/s13148-019-0780-4>.
- Hua, K., J. Zhang, S. Wakana, et al. 2008. "Tract Probability Maps in Stereotaxic Spaces: Analysis of White Matter Anatomy and Tract-Specific Quantification." *Neuroimage* 39, no. 1: 336–347.
- Jensen, D., J. Chen, J. A. Turner, et al. 2023. "Epigenetic Associations With Adolescent Grey Matter Maturation and Cognitive Development." *Frontiers in Genetics* 14: 1222619. <https://www.frontiersin.org/articles/10.3389/fgene.2023.1222619>.
- Johnson, W. E., C. Li, and A. Rabinovic. 2007. "Adjusting Batch Effects in Microarray Expression Data Using Empirical Bayes Methods." *Biostatistics (Oxford, England)* 8, no. 1: 118–127.
- Klingseisen, A., A.-M. Ristoiu, L. Kegel, et al. 2019. "Oligodendrocyte Neurofascin Independently Regulates Both Myelin Targeting and Sheath Growth in the CNS." *Developmental Cell* 51, no. 6: 730–744.e6. <https://doi.org/10.1016/j.devcel.2019.10.016>.
- Knyazeva, M. G. 2013. "Splenius of Corpus Callosum: Patterns of Interhemispheric Interaction in Children and Adults." *Neural Plasticity* 2013: e639430. <https://doi.org/10.1155/2013/639430>.
- Lebel, C., and S. Deoni. 2018. "The development of brain white matter microstructure." *NeuroImage* 182: 207–218. <https://doi.org/10.1016/j.neuroimage.2017.12.097>.
- Lin, D., J. Chen, N. Perrone-Bizzozero, et al. 2018. "Characterization of Cross-Tissue Genetic-Epigenetic Effects and Their Patterns in Schizophrenia." *Genome Medicine* 10, no. 1: 13. <https://doi.org/10.1186/s13073-018-0519-4>.
- Makris, N., J. M. Goldstein, D. Kennedy, et al. 2006. "Decreased Volume of Left and Total Anterior Insular Lobule in Schizophrenia." *Schizophrenia Research* 83, no. 2–3: 155–171.
- Mangiavacchi, A., G. Morelli, and V. Orlando. 2023. "Behind the Scenes: How RNA Orchestrates the Epigenetic Regulation of Gene Expression." *Frontiers in Cell and Developmental Biology* 11: 1123975. <https://www.frontiersin.org/articles/10.3389/fcell.2023.1123975>.

- Moore, L., T. Le, and G. Fan. 2013. "DNA Methylation and Its Basic Function." *Neuropsychopharmacology* 38: 23–38. <https://doi.org/10.1038/npp.2012.112>.
- Mori, S., S. Wakana, L. M. Nagae-Poetscher, and P. C. M. van Zijl. 2005. *MRI Atlas of Human White Matter*. Elsevier.
- Mychasiuk, R., and G. A. S. Metz. 2016. "Epigenetic and Gene Expression Changes in the Adolescent Brain: What Have We Learned From Animal Models?" *Neuroscience & Biobehavioral Reviews* 70: 189–197.
- Perri, F., F. Longo, M. Giuliano, et al. 2017. "Epigenetic Control of Gene Expression: Potential Implications for Cancer Treatment." *Critical Reviews in Oncology/Hematology* 111: 166–172. <https://doi.org/10.1016/j.critrevonc.2017.01.020>.
- Peters, B. D., P. R. Szeszko, J. Radua, et al. 2012. "White Matter Development in Adolescence: Diffusion Tensor Imaging and Meta-Analytic Results." *Schizophrenia Bulletin* 38, no. 6: 1308–1317.
- Pinheiro, J. C., and D. M. Bates. 2000. *Mixed-Effects Models in S, S-PLUS*. Springer.
- Proskovec, A. L., M. T. Rezich, J. O'Neill, et al. 2020. "Association of Epigenetic Metrics of Biological Age with Cortical Thickness." *JAMA Network Open* 3, no. 9: e2015428. <https://doi.org/10.1001/jamanetworkopen.2020.15428>.
- PubChem. n.d. "KCNC1—Potassium Voltage-Gated Channel Subfamily C Member 1 (Human)." Accessed October 13, 2022. <https://pubchem.ncbi.nlm.nih.gov/gene/KCNC1/human>.
- R: MANCOVA. n.d. <https://search.r-project.org/CRAN/refmans/jmv/html/mancova.html>.
- Raudvere, U., L. Kolberg, I. Kuzmin, et al. 2019. "g:Profiler: A Web Server for Functional Enrichment Analysis and Conversions of Gene Lists (2019 Update)." *Nucleic Acids Research* 47, no. W1: W191–W198. <https://doi.org/10.1093/nar/gkz369>.
- Sanchez, C. E., J. E. Richards, and C. R. Almlí. 2012. "Age-Specific MRI Templates for Pediatric Neuroimaging." *Developmental Neuropsychology* 37, no. 5: 379–399.
- Schmidt-Wilcke, T., E. Fuchs, K. Funke, et al. 2018. "GABA—From Inhibition to Cognition: Emerging Concepts." *Neuroscientist* 24, no. 5: 501–515. <https://doi.org/10.1177/1073858417734530>.
- Schneider, E., M. Ditttrich, J. Böck, et al. 2016. "CpG Sites With Continuously Increasing or Decreasing Methylation From Early to Late Human Fetal Brain Development." *Gene* 592, no. 1: 110–118.
- Simmonds, D. J., M. N. Hallquist, M. Asato, and B. Luna. 2014. "Developmental Stages and Sex Differences of White Matter and Behavioral Development Through Adolescence: A Longitudinal Diffusion Tensor Imaging (DTI) Study." *Neuroimage* 92: 356–368.
- Singer, J. D., and J. B. Willett. 2003. *Applied Longitudinal Data Analysis: Modeling Change and Event Occurrence*. Oxford University Press.
- Smith, B. J., A. A. Lussier, J. Cerutti, et al. 2021. "DNA Methylation Partially Mediates the Relationship Between Childhood Adversity and Depressive Symptoms in Adolescence." Preprint, medRxiv. <https://doi.org/10.1101/2021.06.28.21259426>.
- Smith, S. M., M. Jenkinson, M. W. Woolrich, et al. 2004. "Advances in Functional and Structural MR Image Analysis and Implementation as FSL." *Neuroimage* 23, no. S1: 208–219.
- Steinberg, L. 2005. "Cognitive and Affective Development in Adolescence." *Trends in Cognitive Sciences* 9, no. 2: 69–74.
- Stephen, J. M., I. Solis, J. Janowich, et al. 2021. "The Developmental Chronnecto-Genomics (Dev-CoG) Study: A Multimodal Study on the Developing Brain." *Neuroimage* 225: 117438.
- Suzuki, S., N. Ayukawa, C. Okada, et al. 2017. "Spatio-Temporal and Dynamic Regulation of Neurofascin Alternative Splicing in Mouse Cerebellar Neurons." *Scientific Reports* 7, no. 1: 11405. <https://doi.org/10.1038/s41598-017-11319-5>.
- Taylor, P. A., and Z. S. Saad. 2013. "FATCAT: (An Efficient) Functional and Tractographic Connectivity Analysis Toolbox." *Brain Connect* 3: 523–535. <https://doi.org/10.1089/brain.2013.0154>.
- Vuorre, M. 2023. "bmlm: Bayesian Multilevel Mediation." R Package# Version 1.3.13. <https://CRAN.R-project.org/package=bmlm>.
- Wakana, S., A. Caprihan, M. M. Panzenboeck, et al. 2007. "Reproducibility of Quantitative Tractography Methods Applied to Cerebral White Matter." *Neuroimage* 36: 630–644.
- Walton, E., J. Hass, J. Liu, et al. 2016. "Correspondence of DNA Methylation Between Blood and Brain Tissue and Its Application to Schizophrenia Research." *Schizophrenia Bulletin* 42, no. 2: 406–414.
- Wenzel, A., M. Villa, H. Mohler, and D. Benke. 1996. "Developmental and Regional Expression of NMDA Receptor Subtypes Containing the NR2D Subunit in Rat Brain." *Journal of Neurochemistry* 66, no. 3: 1240–1248. <https://doi.org/10.1046/j.1471-4159.1996.66031240.x>.
- Wenzel, A., M. Villa, H. Mohler, and D. Benke. 1996. "Developmental and Regional Expression of NMDA Receptor Subtypes Containing the NR2D Subunit in Rat Brain." *Journal of Neurochemistry* 66, no. 3: 1240–1248. <https://doi.org/10.1046/j.1471-4159.1996.66031240.x>.
- Wheater, E. N. W., D. Q. Stoye, S. R. Cox, et al. 2020. "DNA Methylation and Brain Structure and Function Across the Life Course: A Systematic Review." *Neuroscience & Biobehavioral Reviews* 113: 133–156.
- Williams, A. L., N. Bielopolski, D. Meroz, et al. 2011. "Structural and Functional Analysis of Tomosyn Identifies Domains Important in Exocytotic Regulation." *Journal of Biological Chemistry* 286, no. 16: 14542–14553. <https://doi.org/10.1074/jbc.M110.215624>.
- Zanini, S., L. Martucci, I. Del Piero, and D. Restuccia. 2016. "Cortical Hyper-Excitability in Healthy Children: Evidence From Habituation and Recovery Cycle Phenomena of Somatosensory Evoked Potentials." *Developmental Medicine & Child Neurology* 58, no. 8: 855–860. <https://doi.org/10.1111/dmcn.13072>.
- Zheng, S. C., C. E. Breeze, S. Beck, and A. E. Teschendorff. 2018. "Identification of Differentially Methylated Cell-Types in Epigenome-Wide Association Studies." *Nature Methods* 15, no. 12: 1059–1066.

Supporting Information

Additional supporting information can be found online in the Supporting Information section.

Supplementary Figure: dneu70000-sup-0001-

FigureS1.pdf **Supplementary Tables:** dneu70000-sup-0002-TableS6.pdf